Monitoring of Arc Welding Process Based on Arc Light Emission

Marek Stanisław Węglowski

Additional information is available at the end of the chapter

http://dx.doi.org/10.5772/49987

1. Introduction

A welding process may be expressed as a system shown in Figure 1 whose outputs depends on the welding conditions or their nominal constants (which determine the dynamic model of the system), controlled by the variables or inputs (adjustable welding parameters), and affected by the disturbances (fluctuations or variations of welding conditions from their nominal constants), (Zhang Y.M., 2008).

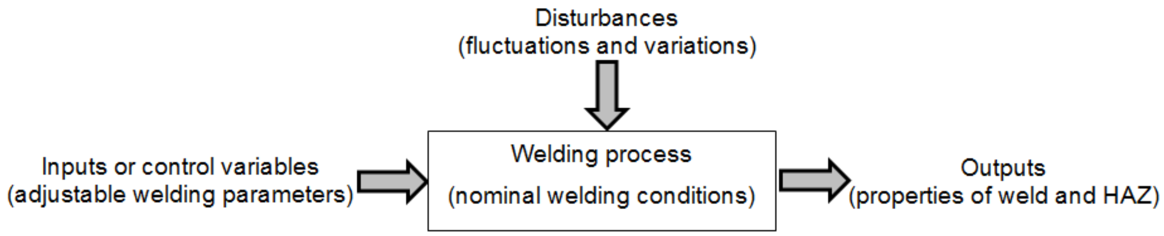

Figure 1. The welding process as a system (Zhang Y.M., 2008)

One of the major goals of the process monitoring in welding is to assure that the required welding parameters are being applied into the process to make a quality of welds. In case abnormal welding parameters are detected, the resultant segment of welds may be post-examined using the more precise methods, (Blakeley P. J., 1990; Siewert T., et al, 1992; Chen X.Q., 2002; Pan J., 2003). This would help to reduce the need of strict/expensive process controls and reduce an extensive use of the costly post NDT (Non-destructive Testing) of all welds. To this end, the monitoring devices are required to be fully automatic and the data analysis of sensed signals including welding parameters and signal generated from the welding arc need to be optimized. In addition, the monitoring devices must also incorporate the criteria so that they can judge if the welds are acceptable or need the additional examinations/repairs.

Monitoring of the welding processes can be divided into the traditional and non-traditional methods (Fig. 2). The traditional methods are based on the monitoring of the electrical and other direct welding parameters, (Kim J.W., et al, 1991; Johnson J.A., et al, 1991; Modenesi P. J., Nixon J.H., 1994; Luksa K., 2006). The non-traditional ones use many different signals, for example: x-ray radiation (Guu A.C., et al, 1992), IR and UV emission (Fan H., et al, 2003), ultrasonic wave (Carlson N.M., et al, 1992), acoustic emission (Taylor-Burge K.L., Harris T.J., 1993) and sound (Saini D., Floyd S., 1998; Luksa K., 2003) to analyse and detect the process.

The traditional methods have been effectively used in the welding process monitoring and control. For example, the measurements of the welding current and arc voltage can be used to estimate the stability of the welding processes, especially with the advanced methods of the signal analysis and AI methods, (Smith J., Lucas B., 1999). The so-called "through the arc sensing", which is based on the measurement and analysis of the welding current and arc voltage, is a widely used traditional method which has been accepted as one of the effective methods for the weld seam tracking. The synergic control of GMAW machines (Amin M., Naseer A., 1987) is also based on the measurements of the current and arc voltage. One interesting case where on-line control of the weld quality is based on the characteristics of the welding arc signal is the narrow groove GMAW with an electromagnetic arc oscillation (Kang Y.H., Na S.J., 2003). The relatively complex plasma arc welding process can be also monitored by using of an electrical signal from the pilot arc (Lu W., Zhang Y.M., 2004). In addition, traditional methods are also useful for detecting of disturbances of the welding process in the form of surface impurities and insufficient shield in GMAW. Monitoring is carried out using specialized monitoring equipment or universal measurement cards.

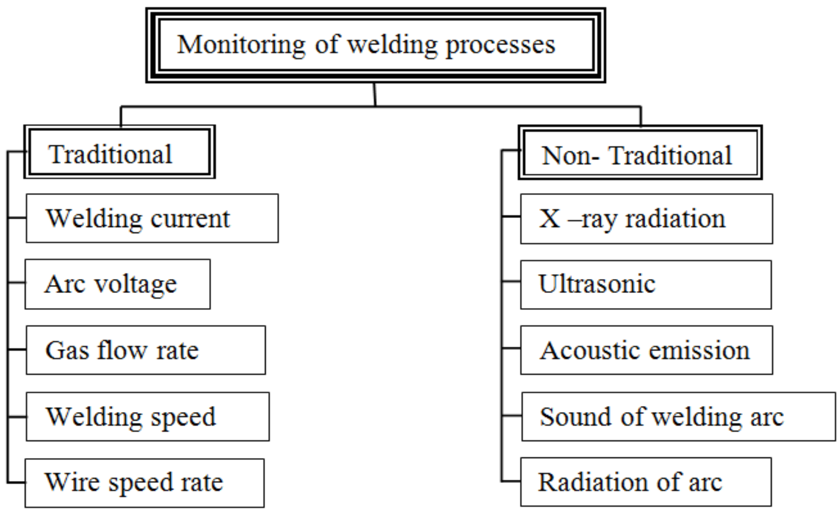

Figure 2. Monitoring methods of welding processes and typical signals

While the traditional methods have advantages of being low-cost and have achieved many successes as aforementioned, many existing issues may require the use of the signals more than the welding current, arc voltage, and the other direct welding parameters. For example, monitoring and control of a weld penetration is an important issue in welding, (Zheng B., et al, 2009) which may require the use of the non-traditional methods. The real-time vision systems take the lead in the non-traditional monitoring methods especially on the robotic welding applications. The CCD (Charge Coupled Devices) video cameras which can be used with the fast algorithms can give us real-time estimates of stability of the process, quality of welds, for example depth of the penetration, (Zhang Y.M., et al, 1993). However, the investment for non-traditional methods is typically high. Cost effective non-traditional methods such as the arc light radiation monitoring which can measure and analyse the intensity of the whole range of the arc light spectrum or intensity of a single emission line (Li P.J., et al, 2001; Wang Q.L., et al, 1997; Yoo C.D., et al, 1997; Ancona A., et al, 2004; Sadek C.A., et al, 2006; Li Z.Y., et al, 2009; Mirapeix J., et al, 2008) are thus desired. This method was first used to determine the length of the arc in the method of MAG in 1966 (Johnson C.A., et al, 1966). The spectroscopy methods are also finding application in the other welding processes such as laser welding (Stabillano T., et al, 2009; Bruncko J., et al, 2003; Kong F., et al, 2012). However, new methods of monitoring require the use of sophisticated measuring equipment, which in most cases need to be adapted for the measurement in welding.

2. Arc light radiation

They are many sources of an electromagnetic radiation of the welding arc area. It can be: the arc column, the regions close to the electrodes, the liquid metal transported across the welding arc, the molten pool, the heated region of the base material around the molten pool, the heated end of the electrode wire ((Pattee H.E., et al, 1973). The welding parameters strongly influence on the range of the wavelength of the electromagnetic radiation and their spectral composition (Hinrichs J.F., 1978). The intensity of the radiation produced by the welding arc is a function of the welding process itself and of the welding variables. The welding arc spectrum can be divided according to wavelength as shown in Table 1. The welding arc in the TIG method are shown in Figure 3.

Type	Wavelength [nm]
Extreme ultraviolet	4 – 200
Ultraviolet	200 – 400
Visible	400 – 750
Infrared	750 – 1300
Far infrared	1300 – Hertzian wavelength

Table 1. Radiation from welding arcs (Hinrichs J.F., 1978)

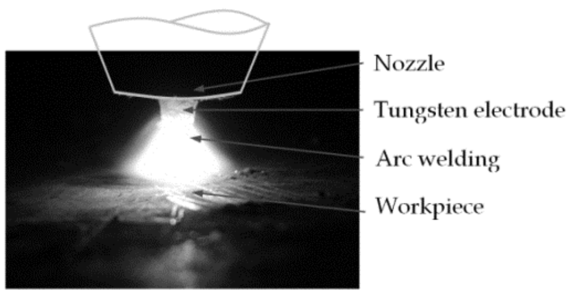

Figure 3. The shape of the TIG arc (welding current 100 A, arc length 2 mm)

The energy dissipated in the arc column is mainly dissipated by the conduction and convection. Emission of an electromagnetic radiation is 10 to 15% of the energy supplied to the arc (Marzec S., Janosik E., 1995). Thermal radiation, whose source is a body of high temperature, is characterized by a continuous spectrum of radiation. The source of the continuous spectrum in the arc is mostly a liquid weld pool (Quigley M., 1977). Radiation characteristics of ions and atoms in the arc is a discrete (Glickstein S., 1976). This type of radiation is analysed in the literature as a plasma radiation.

The plasma at a temperature within the range between several tens of eV and keV (the energy scale 1 eV = 11 600 K) emits an infrared radiation, visible, ultraviolet or X-rays, which, due to the emission mechanism can be divided into the three basic types (Huddlestone R., 1965):

- the line radiation of atoms or ions sent during the move from the one discrete energy level to another (transition between states related);
- the recombination radiation associated with the free-electron uptake by one of the discrete levels of atoms or ions (the transition between the state of the free and associated states);
- braking radiation in the free-electron zone's ion (transitions between free states).

The total radiation of the plasma arc is the sum of a continuous radiation and line radiation of the spectral lines (Szymański A., 1991). This sum can be written as:

$$\varepsilon_{\lambda} = \varepsilon_{\lambda,c} + \sum \varepsilon_{\lambda,L} \tag{1}$$

where: $\varepsilon_{\lambda,c}$ - intensity of radiation with a continuous spectrum, $\varepsilon_{\lambda,L}$ - intensity of spectral lines; sum appearing on the right side of the equation is carried out after all lines lying in the area.

For the optically thin plasma radiation intensity with the continuous spectrum can be written as (Szymański A., 1991):

$$\varepsilon_{\lambda,c} = k_{\lambda,c}(T) \cdot B_{\lambda}(T) \cdot \left(1 - \exp\left(-\frac{hc}{\lambda kT}\right)\right) \tag{2}$$

where: $B_{\lambda}(T)$ - the Planck function for blackbody, $k_{\lambda,c}(T)$ - the total absorption coefficient, T – arc temperature [K], h - Planck's constant ($6{,}6262 \cdot 10^{-34}$ [Js]), c - speed of light in vacuum ($2{,}9979 \cdot 10^{8}$ [ms^{-1}]), λ - wavelength [nm], k - Boltzmann constant $1{,}38 \cdot 10^{-23}$ [JK^{-1}].

The formula for the intensity of the continuous radiation is valid regardless of whether the plasma is in a state of the local thermal equilibrium (LRT) or not. The intensity of a spectral line $\varepsilon_{\lambda,L}$ data is an expression (Szymański A., 1991):

$$\varepsilon_{\lambda,L} = \frac{hcg_q A_{qp} N_e N_i}{8\pi\lambda U_i(T)} \left(\frac{h^3}{2\pi mkT}\right) \cdot \exp\left(\frac{E_{i,q} - \Delta E_i}{kT}\right) \cdot P_{qp}(\lambda) \tag{3}$$

where: g_q – the statistical weight of upper level; A_{qp} – probability of transition; $E_{i,q}$ – ionization energy of the upper level; ΔE_i – decrease of the ionization potential; P_{qp} –line profile, N_e – electron density, N_i – joins density, U_i - the statistical sum of the ion, m – mass of particle.

A spectral distribution and an intensity of the thermal radiation depends on the body temperature. Black bodies with the temperatures up to 500 K emit mostly the infrared radiation at a wavelength > 2 μm. Body with a temperature above about 1000 K, in addition to a long-term infrared radiation also emit the infrared radiation close to the wavelength range 0,78 ÷ 1,4 μm, and very little, because less than 1% of visible radiation. Only body at a temperature higher than 3000 K emits infrared and a visible radiation is also a slightly (0,1%) long-term ultraviolet radiation. Only the body with a temperature above 4000 K emits ultraviolet radiation shorter than 315 nm (Marzec S., Janosik E., 1995). The welding arc radiation intensity is the greatest at the wavelengths between 200 and 1300 nm [16]. The share of the infrared radiation, visible light and ultraviolet radiation in the spectrum depends on the welding method, and the welding parameters (H.E. Pattee, et al, 1973).

The highest intensity of the visible radiation of the arc welding processes is observed in the MIG/MAG and next MMA, TIG and plasma welding. It was also found that the intensity of the ultraviolet radiation increases with the square of the welding current and the intensity of visible radiation is not growing so vigorously (H.E. Pattee, et al, 1973). The intensity of the ultraviolet radiation and visible light emission when welding with the coated electrodes and cored wires (MIG/MAG and self-shielding wires) in the presence of welding fumes is less than that in case of TIG process (for similar welding current). Under the same conditions, the intensity of the infrared radiation does not change dramatically. When a submerged arc welding process is used the visible and ultraviolet radiation is absorbed by a layer of a flux.

Radiation characteristics of the ions and atoms in the arc has a discrete character, and the source of radiation is mainly argon atoms and ions, iron, oxygen and nitrogen. The intensity of radiation of the other elements is much lower. In the wavelength range of the visible radiation spectrum iron, oxygen and nitrogen lines, and only partially spectrum of argon, which the ionization potential is much higher are mainly composed (Petrie T.W., Pfender E. 1970). This also means, that the emission of the light by atoms and ions of argon occurs at the higher temperatures than the temperatures reached at the arc welding for example, in a mixture of $Ar+CO_2$.

The discrete spectral studies provide information about the temperature of the radiation-emitting particles, because the excitation of particles required to provide it with a certain amount of the energy, and for this reason the temperature can be measured. The source of this type of radiation in the arc welding is mainly plasma arc column, but also the metal transported by the arc, slag, and the surface of the welded components (Etemadi K., Pfender E., 1982). The energy regions close to the anode and cathode arc are consumed for heating and melting of the electrode and the base material. It is known that the potential and kinetic energy of the electrons are converted into the surface of the anode heat causing it to intense heat (Petrie T.W., Pfender E., 1970).

The arc radiation is a complex phenomenon and dependent on a number of the welding parameters. To apply for monitoring the radiation of the arc welding process with a high accuracy and reliability is necessary to create the model of the binding intensity of the visible radiation from the arc welding parameters (Yoo C.D., et al, 1997). The welding arc can be regarded as a point source of the radiation. However, this approach in many applications seems to be insufficient. A better approach is to treat the arc as a cylindrical source of the radiation. This model accurately reproduces the actual shape of the welding arc and makes examination of the arc radiation easier. For this reason, it will be elaborated. Cylindrical model can also be simplified and presented as a half-sphere of the welding arc, which is used in the design of the monitoring systems of automated welding process, based on the machine vision systems (Lee C.W., Na S.J., 1996; Yu J.Y., et al, 2003).

Arc column consists of the three types of particles: electrons, ions and neutral atoms. It is assumed that the arc column is in the state of a local thermodynamic equilibrium, in which the electron collisions play an important role in the excitation and ionization.

Equation 2 describes the arc emission of the radiation with a continuous spectrum. Given the relationship between the wavelength and frequency $c / \lambda = \nu$, and the Planck function for the black body, as well as when $h\nu / kT << 1$, the Rayleigh-Jeans'a law is performed. Then the equation 2 can be simplified to:

$$\varepsilon_{\nu} = k'(\nu)\frac{2\nu^2}{c^2}kT_e \tag{4}$$

where: υ - frequence [Hz], T_e - the kinetic temperature of electrons [K].

Compatibility equations 2 with 4 is better than 5% for $\lambda_L T > 4{,}3$ cmK, where λ_L is wavelength [cm]. The right side of equation 4 has a value equal to 1 (approximately) for the infrared and visible radiation. Also, at atmospheric pressure and a normal range of the welding current, the electron temperature is close to the temperature of the arc. Considering the above and apart from the differences in the temperature, it can be eq. 4 write as:

$$\varepsilon_{v} = k'(v)\ \frac{2v^2}{c^2}kT \tag{5}$$

where: T the arc temperature [K].

To simplify the discussion, the gradient of the temperature along the axis of the arc can be omitted. By combining the emission coefficients for the different areas of the arc, the energy radiated from the entire arc can be expressed as:

$$B_{iv} = \iiint \varepsilon_{v} dv \tag{6}$$

After the calculation of the emission factors in the whole arc welding, and after assuming that electrical conductivity and voltage gradient are constant and taking into consideration the impact of visible light weld pool (Zhang Y.M., Li P.J., 2001):

$$B_{iv} = G_1 L I^{\gamma} \left(e^{\frac{G_2}{I}} - \frac{1}{2} \right) + G_3 I^2 + G_4 \tag{7}$$

where: γ, G_i – constants, L – arc length, I – welding current.

Equation 7 gives a relationship between the radiation and the visible arc welding parameters, including the current intensity and the arc length. The authors of the model (Zhang Y.M., Li P.J., 2001) show that this equation is satisfied for arc welding with a current of 150 A, because at the higher currents the current density is not constant over the entire volume of the welding arc.

3. Investigation of the arc electromagnetic radiation

The investigation has been carried out to date focused mainly on examining the luminance of the arc, impact of radiation on the health of the welders (Hinrichs J.F.,1978) and systems to protect them, and to development the tracking systems (torch position). Analysis of the visible light spectrum emitted by the arc welding is used to study the distribution of a temperature in the arc (Farmer A.J.D., Haddad G.N., 1984), calculate the average temperature of the welding arc, an amount of a hydrogen in the shielding gas (Grove L., et al, 1970), and the temperature of molten metal weld pool. The analysis of the arc light emission may help to develop the technique of taking photographs of the welding arc. Spectroscopic methods are a useful tool for studying turbulent shielding gas after leaving the gas nozzle in the TIG and MIG/MAG methods, relationship between the spectral distribution of radiation and the type of a base material and the electron density distribution.

It should be emphasized that the study of the visible radiation in the method of the arc welding MIG / MAG was also used to monitor the metal transfer process in the arc (Wang Q.L., Li P.J. 1997). Methods that use the electrical signals (measure the welding current and arc voltage) are effective only to track the short arc and globular metal transfer welding process. When the metal is being transferred by the spray mode, the signal / noise ratio is too small, and the greater accuracy is achieved by measuring the intensity of the visible radiation arc (Wang Q.L., Li P.J., 1997). Optical methods are also applied to scan the length of the welding arc in the TIG and the MIG/MAG methods.

In parallel, a wide range of plasma research is conducted. First of all, emission spectroscopy and scattering of a laser radiation (laser spectroscopy) were used. These methods allow the calculation of plasma parameters such as a temperature and concentration of atoms (ions, electrons).

The emission spectroscopy is a passive method in which the electromagnetic radiation from the plasma (one or many spectral lines) is recorded and analysed. The advantage of this method is particularly simple measurement. This requires an optical focusing system, a monochromator or a spectrometer and detector, which can be photomultiplier or CCD. The disadvantage of this method is that the recorded radiation is a total emitted from the plasma. In order to obtain measurement data from one particular point of the measurement, it is necessary to use the Abel transformation (Cho Y.T., Na S.J., 2005). Another disadvantage is the need to run the calculation assumptions that the plasma is in a state of a local thermodynamic equilibrium and is optically thin.

Laser spectroscopy is a more universal method. However, it requires a laser light source and a detection system. The method of the laser spectroscopy allows for determination of the plasma parameters at a given point. In some cases, calculation of the plasma parameters without the assumption that the plasma is in thermodynamic equilibrium allowed. This technique uses: the Rayleigh scattering, Tomson scattering, laser induced fluorescence (LIF) and two photon laser induced fluorescence.

Plasma radiation recorded in the measurements perpendicular to the axis of discharge (called side-on) is the sum of the smaller contributions from the various layers of plasma (Figure 4). The known Abel transformation (Cho Y.T., Na S.J., 2005) allows to determine ε(x) knowing I(x).

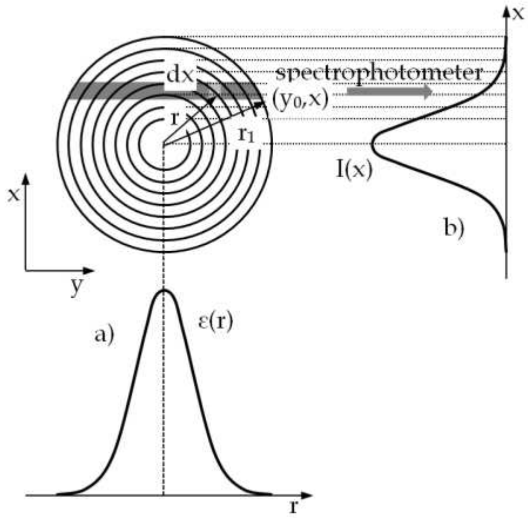

Figure 4. Cross section of the plasma column, the discharge axis is perpendicular to the plane of the paper, A - radial distribution of the emission factor, B - distribution of intensity observed on the side, I(x) - radiation distribution of intensity in the plane perpendicular to the direction in which the plasma is observed, x – distance from the direction of observation of plasma (Cho Y.T., Na S.J., 2005)

If the plasma in the observed cross-section is cylindrically symmetrical and the phenomenon of self-absorption does not occur, the radiation distribution of intensity in the plane perpendicular to the direction of observation of the plasma can be determined by the formula (Cho Y.T., Na S.J., 2005):

$$I(x) = 2 \cdot \int_x^{r_0} \frac{\varepsilon(r) \cdot r}{\sqrt{r^2 - x^2}} \, dr \qquad (8)$$

where: ε(r) – intensity of radiation emitted by the plasma per unit thickness or distant from the axis of the discharge, x – distance from the direction of observation of plasma (Fig. 4), $2r_0$ – diameter of the area in which the plasma occurs.

Up to now, the main goals of the plasma investigation in the welding arc were creation the mathematical and physical models of the arc (Fan H.G., et al, 1997). These models will be very useful to design new welding machines. Very important aspect of experiments is to find the correlation between the electric welding parameters and the properties of the welding arc. Many experiments concern studies about the influence the composition of the shielding gas on the plasma properties. Also some investigation concern a magnetic arc deflection (Kang Y.H., Na S.J., 2002). The most important aim of investigation is to calculate the arc efficiencies. Many experiments were focus on the physical properties of the plasma welding arc, for example the temperature distribution, velocity fields of the electrons and ions, electrode work functions, and the local thermodynamic equilibrium in free-burning arcs in argon. Modern methods of welding, including A-TIG method, prompted the author (Ogawa, Y. 2004) to study the effect of the additional elements and compounds intentionally introduced to the area of the welding arc on properties.

In a study of the arc radiation it is important to determine the influence of individual factors on the width of the spectral peaks. Typical spectral line profile is shown in Figure 5 together with the characteristic values: x_c – wavelength of the center line, FWHM - Full Width at Half Maximum, I_{max} – maximum value for the radiation intensity of spectral line. The natural width of the spectral lines (Huddlestone R.H., Leonard S.L., 1965) is due to the finite lifetime of the energy levels and is higher, the lifetimes are shorter. Emission line profile resulting from natural broadening is the Lorentz distribution.

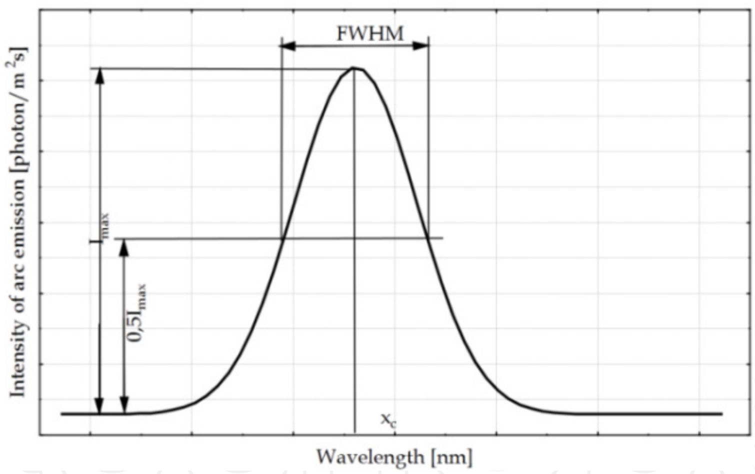

Figure 5. Typical spectral line profile

The second important factor is the Doppler broadening of the spectral lines, which is associated with the movement of the particles emitting the radiation. If the emitter has a velocity component of the direction consistent with the observation, the relative change in wavelength, involve a change in frequency is called Doppler effect. In the case of a thermal motion when emitting particle velocity distribution is Maxwell's distribution, the profile of the emitted spectral line is the Gaussian profile (Zielińska S., 2004).

Another kind of broadening, which can be encountered in the analysis of spectral lines, is a pressure broadening. This kind of broadening of the spectral line is the result of collisions with the other particles emitter. They can limit the lifetime of the excited atomic levels, and thus lead to an broadening of the line profile, which in this case is the Lorentz distribution. There are basically three types of the pressure broadening: the resonances, van der Waals and Stark (Zielińska S., 2004).

Components of the measurement system is a factor caused the further broadening of the spectral line. Apparatus profile in this case is the Gaussian profile. Theoretically, the spectrometer apparatus function should be linearly dependent on the wavelength. In reality, however, the profile apparatus is a convolution of functions associated with the matrix detector and functions of the optical elements of the spectrometer (Zielińska S., 2004).

The factors leading to the broadening of the spectral lines can be divided into given the Lorentz and Gaussian profiles. Their impact on the value of the broadening is different and may depend on conditions in the plasma. Resultant spectral line profile is a function which is a convolution of the Lorentz and Gauss functions (Huddlestone R.H., Leonard S.L., 1965) called the Voigt profile.

It should be noted that the photo-detector (CCD detector), in addition to the signal, measures also the background radiation. To eliminate the influence of background radiation, when analysing the intensity distribution of the welding arc radiation this radiation must be subtracted.

Taking into account the resolution of the transmitters, the recorded peaks are "cluster" of several spectral lines of a single element (Fig. 6), or even a few elements in the various degrees of ionization. So, matching the shape function is important in determining the exclusion of gravity for that group of peaks. The first element of the monitoring system of welding processes is to develop methods for the identification and measurement of the characteristic quantities of recorded spectral line, such as a peak width, position and amplitude of maximum. The examination which function better describes the profile of the peak ("cluster" of spectral lines) seems to be crucial for the detection of disturbances of the welding process. Profiles of the peaks can be matched using Gaussian, Lorentz and Voigt functions (Fig. 6).

Matching functions are carried out mostly using the least squares method (eg. Levenberg-Marquardt algorithm) and special software can be adapted for this purpose. On the basis of the matching function parameters the position of maximum spectral line (xc) and the spectral line width (FWHM) can be determined. In developing the experimental data even in so-called matching additive constant y_{00} must be considered. The constant is present due to the additional signals recorded by the measurement apparatus.

From the equation (7), a relationship between intensity of the welding arc radiation (energy radiated for a given spectral line xc) B_{iv}, arc length and welding current can be designated. Using a software, coefficients G_i and γ can be estimated basing on the collected data.

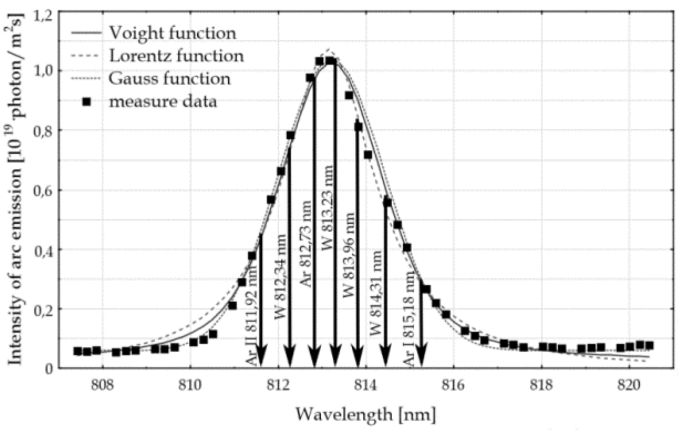

Figure 6. An example of peak matched Gaussian functions, Lorentz and Voigt, I=200 A, L=3 mm, 100 % Ar with marks of spectral lines .

The values of the parameters characterizing the welding process can be determined minimizing the sum of squares:

$$\chi^2 = \sum_l \sum_k \frac{1}{\left(\Delta B_{kl}\right)^2} \left[B_{kl}\left(I_k, L_l, \lambda\right) - \tilde{B}_{kl}\left(I_k, L_l, \lambda, \{g_i\}\right)\right]^2 \tag{9}$$

where: I_k – welding current; L_l – arc length; $B_{kl}(I_k, L_l, \lambda)$ - intensity of light of wavelength λ recorded during the welding current I_k, at arc length L_l; ΔB_{kl} - uncertainty set of light intensity $B_{kl}(I_k, L_l, \lambda)$; $\tilde{B}_{kl}$ $(I_k, L_l, \lambda, \{g_i\})$ - defined by formula (7) the theoretical intensity of the light with a wavelength λ recorded during the welding current I_k, at arc length L_l; $\{g_i\}=\{G_1, \gamma, G_2, G_3, G_4\}$ - set of values of the parameters appearing in formula (7).

Uncertainty-determination and the parameter $g \in \{g\} = \{G_1, \gamma, G_2, G_3, G_4\}$ is determined by the method described in (Kończak S., Nowak M., 1981):

$$\varepsilon_i = \frac{\chi^2}{m_p - m} h_{ii}^{-1} \tag{10}$$

where: h_{ii}^{-1} - ii component of the inverse Hesse matrix; χ^2 - sum of squared deviations from the theoretical value of the experimental results; m_p- number of experimental results; m-number of parameters designated by the matching.

The components of the Hesse matrix model is defined as (Kończak S., Nowak M., 1981):

$$h_{ij} = \frac{\partial^2 \chi^2}{\partial g_i \partial g_j} = -2 \sum_l \sum_k \frac{1}{\left(\Delta B_{kl}\right)^2} \left[\begin{array}{l} B_{kl}\left(I_k, L_l, \lambda\right) \dfrac{\partial^2 B_{kl,teor}\left(I_k, L_l, \lambda, \{g_i\}\right)}{\partial g_i \partial g_j} - \dfrac{\partial B_{kl,teor}\left(I_k, L_l, \lambda, \{g_i\}\right)}{\partial g_i} \\ \dfrac{\partial B_{kl,teor}\left(I_k, L_l, \lambda, \{g_i\}\right)}{\partial g_j} \end{array} \right] \tag{11}$$

4. Application of the arc light emission to monitor the welding process

In order to monitor the welding processes successfully, the optical sensing systems have been developed. Special procedures, models and modification of the monitoring devices have to be implemented with the sensing systems, some of the systems are discussed herein. Some typical application examples included sensing of the arc length in the TIG welding (Węglowski M.St., 2010), relationship between the welding conditions and intensity of the arc light emission in the MIG/MAG methods (Węglowski M.St., 2008; Węglowski M.St., Zhang Y. M., 2010) and the influence of the parameters and disturbance of the welding process on the shape of the spectrum of the arc light radiation (Węglowski M.St., 2009). In this part, their principles are being described.

4.1. Sensing of the arc length in the TIG welding method based on the arc light intensity

One of the main task of the monitoring systems in the robotized and automated welding stations is the measurement and control of the arc length. The main objective of the investigation was to study the possibilities of using of the visible radiation of the welding arc for stability monitoring of the TIG welding process, giving consideration to the changes of the intensity of visible light radiation with the changes of the welding current or welding arc length (reproducing the case of burn- through and arc migration). The arc length is one of the basic welding parameter in the TIG method, which directly influences the arc voltage. The arc length has an effect on the distribution of an arc energy, and as the consequence on the amount of heat put into the welded joint and on the width of the weld.

The tests have been performed on the stand for the automatic TIG welding. The measuring system consists of welding current and voltage transducers, an electrooptical converter, a measurement card and a PC computer. The analysed beam of the visible radiation is fed into the electrooptical converter by means of a standard optical wave guide. The electrical signal corresponding to the visible light intensity and signals from the welding circuit are recorded on the PC by the recording device, equipped with the NI DAQ 6036 measuring card. The recorded signals were then analysed. The intensity of the visible light radiation of the welding arc was measured in volts. The following experiment conditions were approved: the arc burns between the thoriated tungsten electrode (cathode) and a copper plate (anode), the welding torch is fixed, argon (Ar) as the shielding gas (gas flow rate q_g=10 dcm^3/min), welding current source: Kemppi Pro 5000 (DC current set in the range of 30÷300 A). It was assumed that the arc length is equal to the distance between the electrode tip and the welded metal surface. The range of the welding arc length L=2÷5 mm. In Figure 7 show the configuration of the optical system relative to the welding torch is shown.

The arc length was changed in the range from 2 to 5 mm during the experiments. Figure 8 shows the influence of the arc length L on the visible light intensity and arc voltage for the welding currents in the range of 50÷300 A. It can be seen that considerable changes of the arc length are followed by the substantial changes of radiation intensity of the welding arc (wave length 696 nm) and only by small changes of the arc voltage.

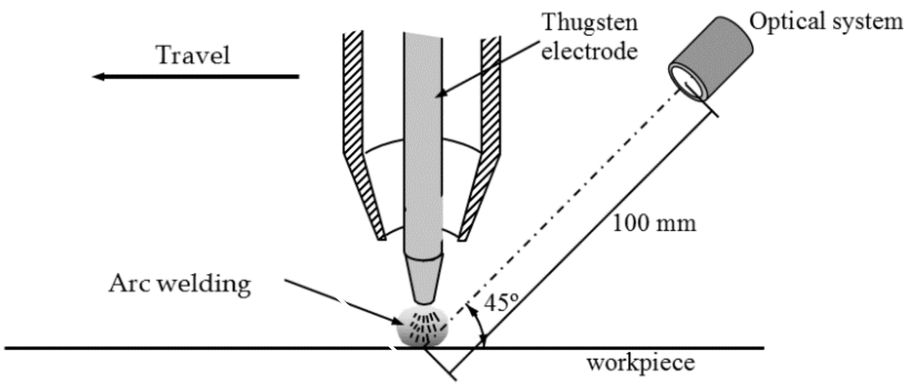

Figure 7. Configuration of the optical system relative to the welding torch

Three cases of transient states of the welding arc length have been also investigated: the abrupt change of the arc length (Fig. 9a), the abrupt change of the welding arc length, simulating the burn-through of the joint (Fig. 10a) and a smooth change of the welding arc length, simulating a bad preparation of welded elements or their distortion during welding (Fig. 11a). These are typical transient states in the welding practice.

The abrupt change of the welding arc was forced by a proper preparation of the 20 mm thick plate by milling (Fig. 9a). The height of the received steps was 1 and 2 mm, which resulted in the arc length of 1, 2 and 4 mm at a welding current of 100 A (DC). Results of the measurement performed at the welding speed of 60 cm/min are presented in Figure 9b. The moment of entering the step by the welding torch is shown by arrows.

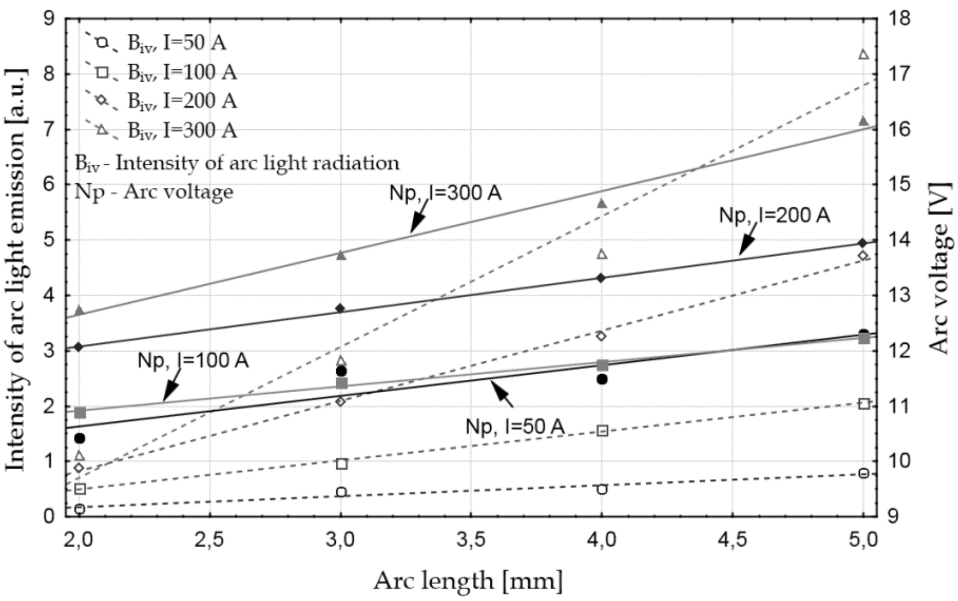

Figure 8. Influence of welding arc length on the light emission (B_{iv}) and the arc voltage (N_p) at the welding current in the range of 50÷300 A. Argon as shielding gas

The second tested transient state was the abrupt change of the arc length simulating the burn-through of the welded joint. A 20 mm thick plate were prepared by drilling holes with a diameter of 1,3÷6 mm (Fig. 10a). The arc length during the experiment was maintained at 3 mm at the

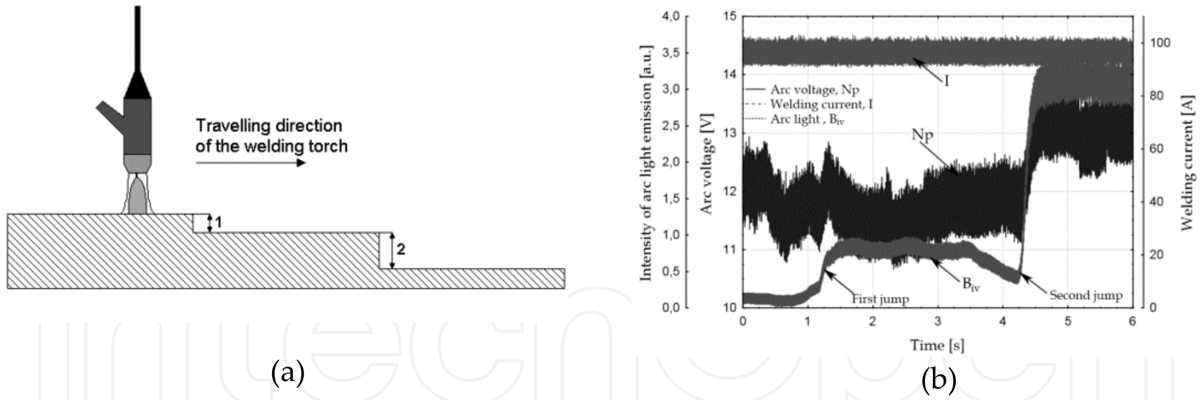

Figure 9. (a) scheme of the experiment with the forced abrupt change of welding arc length, (b) measurement results of the welding current, arc voltage and intensity of arc radiation at abrupt changes of the welding arc length, welding speed 60 cm/min

welding current of 100 A (DC) and a welding speed of 60 cm/min. The test results are presented in Figure 10b. The moment of entering the holes by the welding torch is shown by arrows.

The third tested transient state was a smooth change of the arc length simulating the deformation of welded plates or improper preparation of the joint. Plates 20 mm in thickness were welded at the angle of 5° (Fig. 11a). The arc length during the experiment changed in the range of 1÷7 mm at the welding current of 100 A (DC) and a welding speed of 60 cm/min. The test results are presented in Figure 11b.

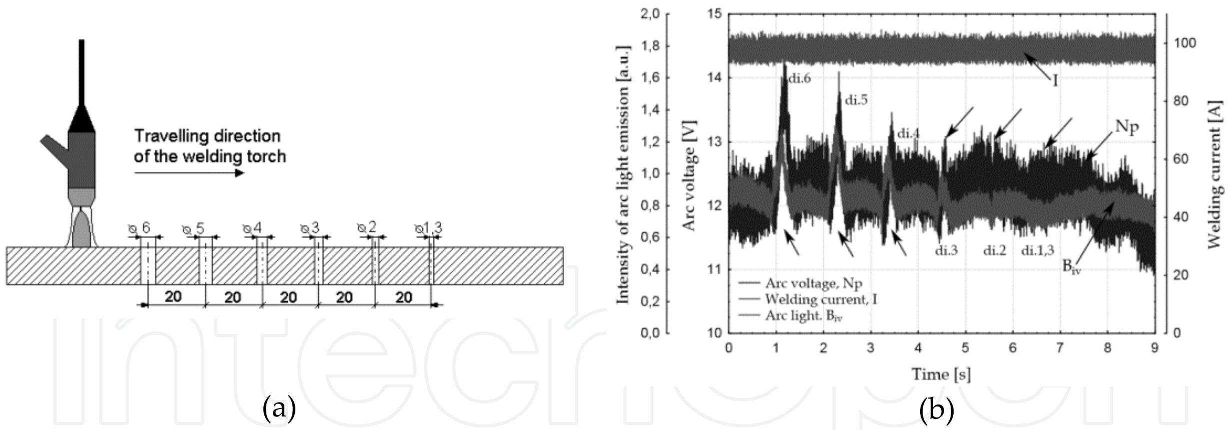

Figure 10. (a) scheme of the experiment with the forced abrupt change of welding arc length simulating the burn-through of the welded joint, (b) measurement results of the welding current, arc voltage and intensity of arc radiation at abrupt changes of the welding arc length simulating the burn-through of the welded joint, welding speed 100 cm/min,

The one of the most important factor is the influence of the changes of welding current and the arc length during TIG welding on the intensity of the visible radiation. On the basis of the collected test data and equation 2 a relationship combining the intensity of the welding arc radiation (B_{iv}) with the arc length (L) and the welding current intensity (I) can be determined. The arc length is in the range of 2 ÷ 5 mm. Based on the formula (7) presented in the paragraph the relationship can be determined. Using a software, basis of the collected data and formulas (9-11), coefficients G_i and γ can be estimated.

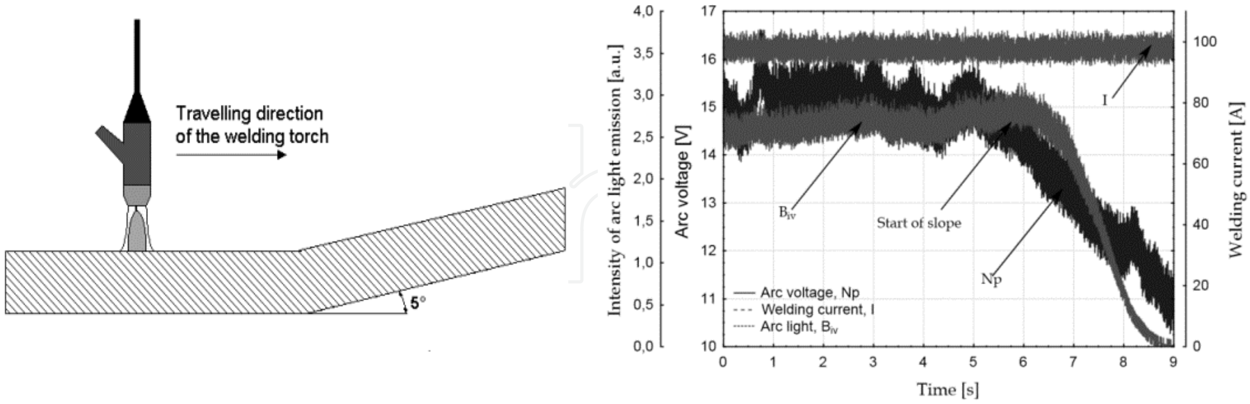

(a) (b)

Figure 11. (a) scheme of the experiment with the smooth change of the welding arc length simulating improper preparation of the joint or deformation of welded plates, (b) measurement results of the welding current, arc voltage and intensity of the arc radiation at the smooth change of the welding arc length, welding speed 60 cm/min

Two cases were taken into account during calculation:

- theoretical Zhang model, in this model coefficient γ=2 and then it can be written (eq. 7):

$$B_{iv} = G_1 L I^2 \left(e^{\frac{G_2}{I}} - \frac{1}{2} \right) + G_3 I^2 + G_4 \qquad (12)$$

- generalization model - coefficient γ is a parameter dependent on the measured data.

Basing on the formula (9) the calculation were carried out taking into account the following two cases:

- ΔB_{kl} - uncertainty set of the light intensity is constant for all data and it is not taken into account during calculations; in this case the fitting will be worse for smaller values,
- ΔB_{kl} - uncertainty set of the light intensity is not constant for all data and it is taken into account during calculations.

No	Coefficients	Theoretical model	Generalization model
1	G1	$3,8(2)\cdot 10^{-5}$	$1,11(1)\cdot 10^{-3}$
2	G2	56(3)	9(2)
3	G3	$-4,4(1)\cdot 10^{-5}$	$-3,98(12)\cdot 10^{-5}$
4	G4	$1(57)\cdot 10^{-3}$	$-1,8(6)\cdot 10^{-1}$
5	γ	2	1,455(4)
6	χ^2 sum of the least-squares of the deviations	7,33	3,6
7	correlation coefficient R_2	0,98	0,99

Table 2. Results of calculation of coefficients G_i for theoretical and generalization models at arc length in the range of 2 - 5 mm, ΔB_{kl} – constant

No	Coefficients	Theoretical model	Generalization model
1	G1	$4,6(2)\cdot 10^{-5}$	$1,7(1)\cdot 10^{-3}$
2	G2	34(2)	$2(65)\cdot 10^{-2}$
3	G3	$-4,06(10)\cdot 10^{-5}$	$-35,1(6)\cdot 10^{-6}$
4	G4	$-1,09(16)\cdot 10^{-1}$	$-11,4(9)\cdot 10^{-2}$
5	γ	2	1,364(2)
6	χ^2 sum of the least-squares of the deviations	5,75	1,07
7	correlation coefficient R^2	0,99	0,99

Table 3. Results of calculation of coefficients G_i for theoretical and generalization models at arc length in the range of 2 - 5 mm, ΔB_{kl} – is not constant

Taking into account the results given in Tables 2 and 3, the sum of the least-squares of the deviations is smaller for the generalization model and for case were weight ΔB_{kl} is not constant. Finally the formula 9 can be written as:

$$B_{iv} = 0,0017 L I^{1,364}\left(e^{\frac{0,02}{I}} - \frac{1}{2}\right) - 0,000035 I^2 - 0,114 \qquad (13)$$

This equation is satisfied for the wavelength 698 nm and the arc length in the range of 2 - 5 mm. The graphic presentation of this formula is shown in Figures 12a and 12b. The arc burns between the thoriated tungsten electrode (cathode) and a water cooled copper plate.

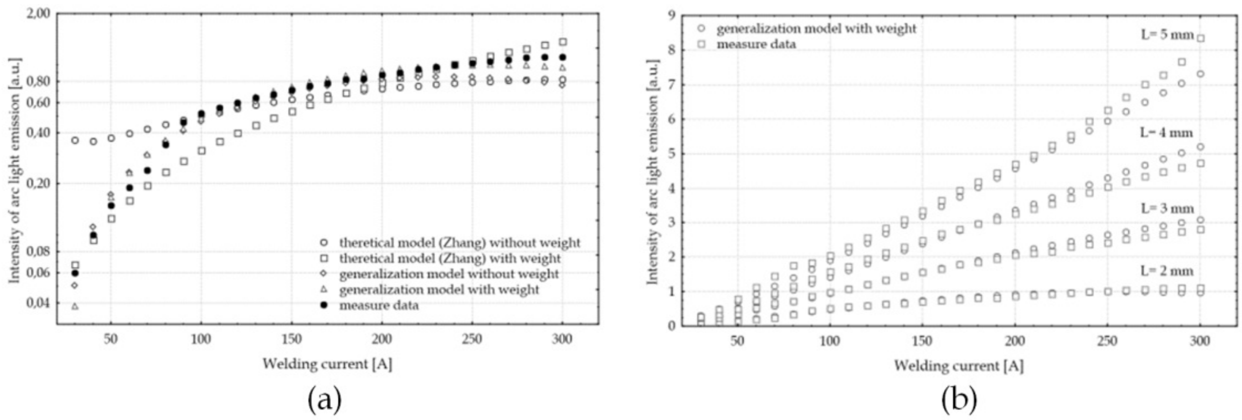

Figure 12. (a) relationship between intensity of the welding arc radiation in the TIG method and welding current at arc length 2 mm, and the wavelength 698 nm, (b) relationship between an intensity of the welding arc radiation in the TIG method and the arc length, welding current at arc length in the range of 2-5 mm, and the wavelength 698 nm

The change of the TIG welding arc length causes also changes of the intensity of the visible arc radiation. An increase of the arc length results in the intensity increase of the selected spectral line (696 nm) of the TIG welding arc visual radiation. This increase depends on the welding current intensity. Larger increases of the visual arc radiation intensities are observed at the higher welding currents.

Three cases of the welding arc length transient states have been tested. It has been found that in all that cases the intensity of the arc radiation at the wave length of 696 nm is much more sensitive to abrupt changes of the welding arc length, than the arc voltage. In the first case (Fig. 9) the change of the arc length for 1 and 2 mm was followed by a 400% change of the radiation intensity and only by a 10% change of the arc voltage. In the second tested case, simulating the burn-through of the welded joint, considerable changes take place for both - the arc voltage and intensity of the arc radiation, but in the radiation intensity record the peaks corresponding to the consecutive holes (Fig. 10) can be more easily identified. By the arc voltage measurement a hole with a diameter of 4 mm can be identified, while the measurement of radiation intensity makes possible the identification of a 1,3 mm hole. The third tested transient state was a smooth change of the welding arc length, simulating the deformation of welded plates or incorrect setup for welding. Also in that case the changes of the welding arc length are followed by considerable changes of radiation intensity and smaller changes of the arc voltage.

4.2. Relationship between the welding conditions and intensity of the arc light emission in GMAW

This section describes the acquisition and analysis of the arc light emission and its correlation with the welding parameters and disturbances of the welding process. A spectrophotometer card PCI 2000 ISA-A in the visible spectral range of 340 nm to 860 nm was used in the study. The measurement system consisted of the welding current and voltage transducers, an electro-optical converter, a data acquisition card and a PC computer (Fig. 13). Signals from the welding circuit were recorded on the PC through the data acquisition card NI DAQ 6036. The measurements during bead-on-plate welding and joints welding were carried out. The signals were analyzed in time domain. During trials, a spectrophotometric card PCI 2000 ISA-A, which has been designed for the CCD Sony model ILX511 detector in the visible spectral range of 340 nm to 860 nm was used to image and record the arc light spectrum for the later analysis. The CCD detector was a line scan array of 2048 pixel.

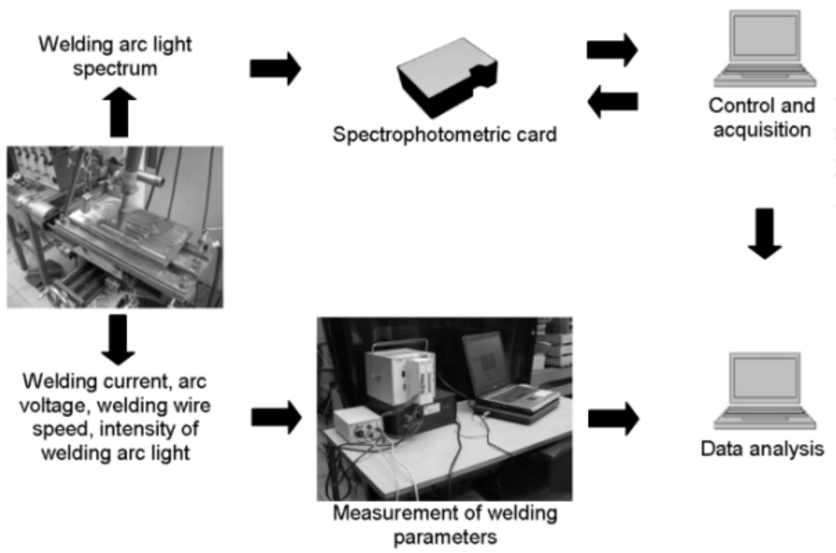

Figure 13. Experimental setup with the flow of data

The work-piece was moved while torch was in a fixed position such that the arc light sensor was stationary in relation to the work-piece. The sepctrophotometric card used a sampling time 3 ms. An optical system was used to focuse the welding arc light. The entire arc column has been analyzed as a single object. During welding the arc voltage, the welding current, the wire feed speed and the intensity of the arc light emission were continuously measured. The Hall effect current sensor Model PR 1001 was used to measure the welding current. This sensor provides electrical isolation between the current carrying conductor and the output of the sensor. The voltage was measured by a resistance bridge by a LV 25 P transducer in the output of the power supply. The wire feed speed was measured by E21 MPL10 transducer. The intensity of the arc light emission was measured by PIN BPW34 photodiode. Signals from the welding circuit were recorded on the PC through the IPP-2 measured system designed in the Instytut Spawalnictwa (Institute of Welding), witch based on SCXI data acquisition system National Instruments. This system consisting of the National Instruments SCXI-1125 is 8-channel isolated analog input modules and data acquisition board NI DAQ 6036 E. Whole system was placed in the SCXI-1000 chassis. The signals were recorded at a sampling rate of 20 kHz.The torch was moved at the travel speed 25 cm/min to make bead-on-plate welds and weld. Direct current levels between 104 A and 235 A were examined, all at an operating voltage in the range of 16.5 V - 25.5V. Figure 14a shows the arc spectrum obtained in the range of 360-860 nm at the welding current in the range of 104 – 235 A. The graph is presented in a logarithmic scale.

As shown in Figure 14a the increase of the welding current causes increase of the arc light intensity in the whole range. The shape of the spectrum was modeled by the three mathematic functions: Lorentz, Gausse and Voight (Fig. 14b). The fitting for both single wavelength and multiple wavelengths was carried out mathematically and the best result was achieved with the Lorentz function. The central wavelength, intensity and FWHM - Full With at Half Maximum were calculated. The main source of the arc light radiation in the GMAW is liquid metal. The lines from the shielding gases have not been found. The detailed analysis of influence of the welding current on the arc light spectrum was previously discussed (Węglowski M.St., 2008, 2009).

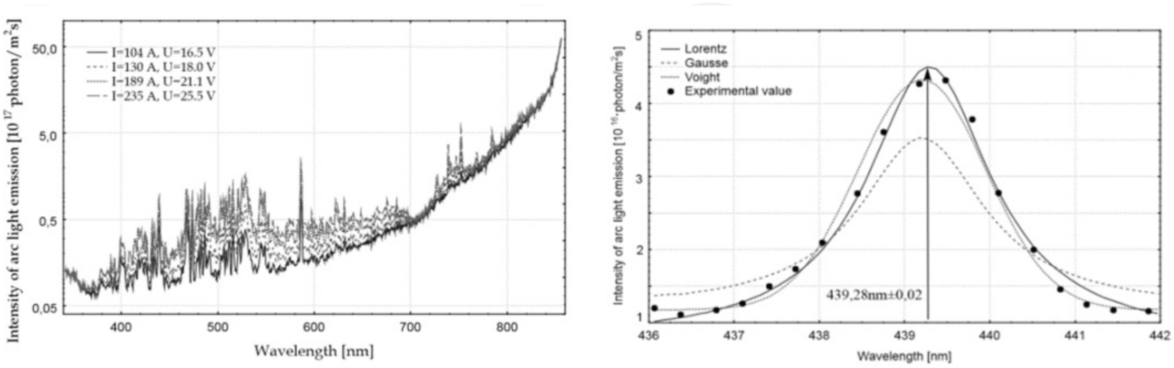

(a) (b)

Figure 14. (a) effect of the welding current on the arc light spectrum. The welding current in the range of 104-235 A, Ar + CO_2 as the shielding gas, wavelength in the range of 480-860 nm. Logarithmic scale, (b) calculated line profile of the wavelength 439,28 nm compared with measured values and the Gaussian, Lorentz and Voight functions

The purpose of these studies was also to check the influence of disturbances of the welding process on the arc light intensity. To this end, arc light intensity was measured during welding of real joint, 4 mm in thickness. The disturbances of the welding process was tha additional filler metal in the grove. The experiments were done under the following conditions: welding current I=160 A, arc voltage U=21.2 V, shielding gas M21 Ferromix C18, welding speed 25 cm/min), wire EN 440 G3Si1, base material S235, the grove was prepared for Y.

The weld produced is shown in Figure 15a. The scheme of the method of disturbance of the welding process is shown in Figure 15b. The macroscopic examination of the padding welds are shown in Figure 16. During welding the arc voltage, welding current, wire feed speed and the intensity of the arc light emission were continuously measured. The intensity of the arc light signal is shown in Figure 17.

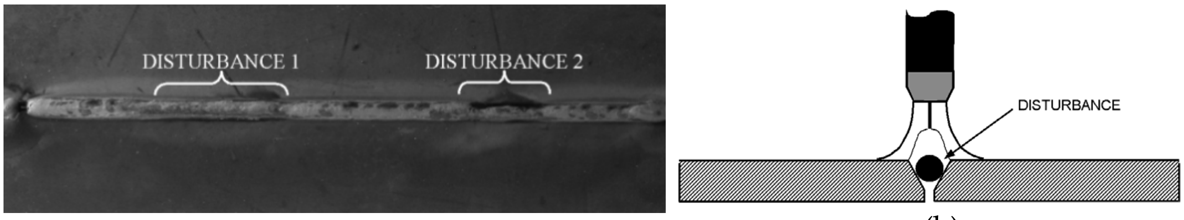

(a) (b)

Figure 15. (a) welding joint with marked areas of disturbances of the welding process, (b) scheme of disturbance of the welding process

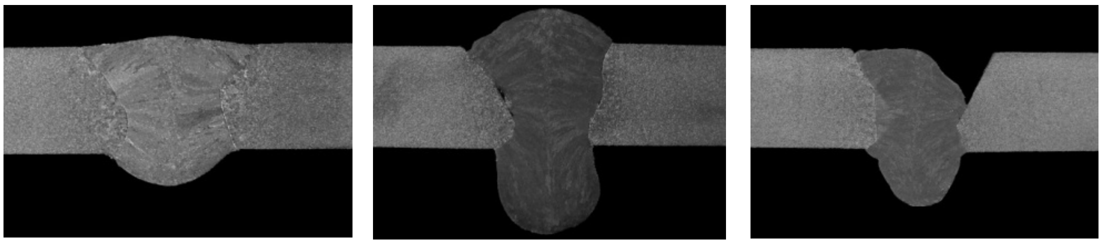

(a) without disturbances

(b) disturbance 1

(c) disturbance 2

Figure 16. Macroscopic examination of the padding welds. Etching Adler, magnification x2

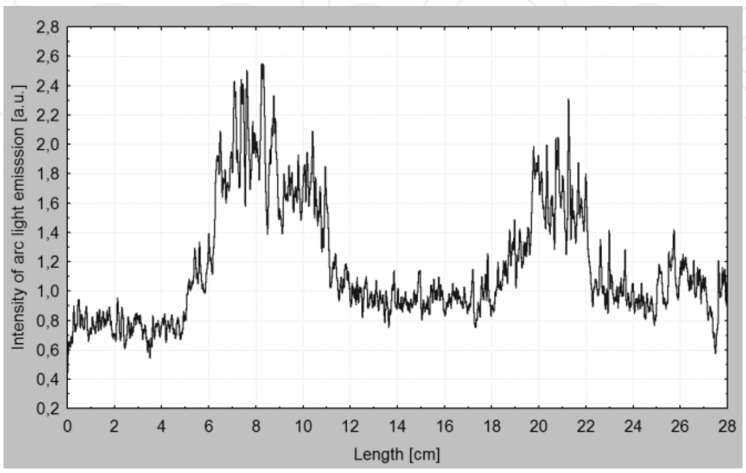

Figure 17. Intensity of the arc light signal recorded during welding of plate with disturbance

To estimate the stability of the welding process based on the arc light emission the least squares method was used. To model the arc light signal a cubic polynomial was used:

$$y = a_0 + a_1 x + a_2 x^2 + a_3 x^3 + \varepsilon \tag{14}$$

where: y – arc light emission, x – time, a_i – coefficients, ε – residual the differences between the observations and the model.

To calculate a residual the following formula should be solved:

$$Y = \begin{bmatrix} y(m-M \\ . \\ y(m) \\ . \\ y(m+M \end{bmatrix} \quad X = \begin{bmatrix} 1 & x(m-M & x^2(m-M) & x^3(m-M) \\ . & . & . & . \\ 1 & x(m) & x^2(m) & x^3(m-M \\ . & . & . & . \\ 1 & x(m+M) & x^2(m+M) & x^3(m+M \end{bmatrix} \quad \beta = \begin{bmatrix} a_0 \\ a_1 \\ a_2 \\ a_3 \end{bmatrix} \tag{15}$$

where: Y- intensity of the arc light signal matrix, X – time matrix, β – coefficients matrix, m – discrete time.

But this system is over determined. There are more equations than unknowns. So it cannot expect to solve the system exactly. Instead, it can be solved it in the least squares sense:

$$\min_\beta \|X\beta - Y\| \tag{16}$$

A theoretical approach to solve the over determined system begins by multiplying both sides by XT. This reduces the system to a square, *n*-by-*n* system known as the normal equations:

$$X^T X\beta = X^T Y \tag{17}$$

If there are thousands of observations and only a few parameters, the design matrix X is quite large, but the matrix $X^T X$ is small. It has been projected Y into the space spanned by the columns of X. Continuing with this the theoretical approach, if the basis functions are independent, then $X^T X$ is nonsingular and

$$\beta = \left(X^T X\right)^{-1} X^T Y \text{ and } \overline{Y} = \overline{X}\beta \tag{18}$$

then, the residual can be calculated as:

$$\varepsilon = \sqrt{\sigma^2} = \sqrt{\frac{\left(Y - \overline{Y}\right)^T \left(Y - \overline{Y}\right)}{2M+1}} \tag{19}$$

where: 2M+1 – the number of data used in the fitting.

To calculate formulas 15 and 19 the following parameters were established: m in the range of 10000 to 590000 at the step 100 and M=10. To estimate the points of unstability of the welding process, model by polynomial can be used. To estimate the best degree of the polynomial the F-test method can be used. Based on the previously least squares methodology, the residual of polynomials ε_P can be calculated as:

$$\varepsilon_P = \sqrt{\sigma^2} = \sqrt{\frac{\left(\varepsilon - \bar{Y}\right)^T \left(\varepsilon - \bar{Y}\right)}{n}} \tag{20}$$

where: ε – residual from eq. 7, Y – value of polynomial function, n – the number of data.

The calculation acc. to formula 20 were carried out for 50 different polynomials. The best results can be achieved for polynomial 28th degree (Figure 18).

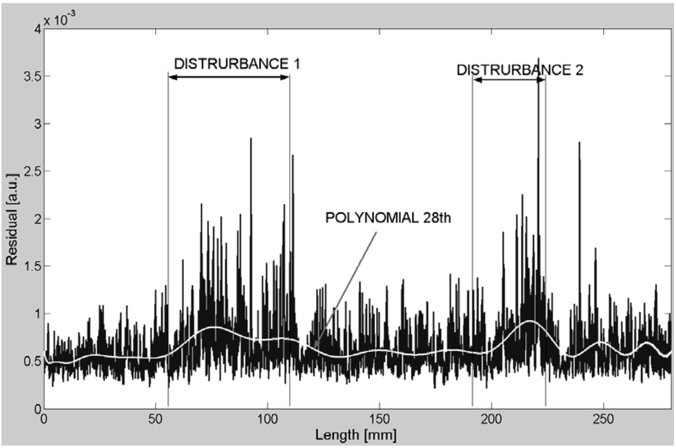

Figure 18. The results of model by polynomial 28th degree with marked the areas with disturbances.

It is shown that the arc light signal can be utilized to monitor the welding processes. This signal is sensitive to any changes in the welding area. The spectrophotometric card can be useful tool to investigate the properties of the welding arc.

4.3. The influence of the parameters and disturbance of the welding process on the shape of the spectrum of the arc light radiation

The tests were performed on the stand for automatic MAG welding operations by the control consol. The testing plate for welding was fixed while the welding was moved at a controlled speed. The torch was located perpendicularly to the welding surface. All experiments were performed by the bead-on-plate welding. The measuring system consisted of the welding current and the voltage transducers, a PC computer equipped with the CCD spectrophotometer card, and a speed wire measurement device. The electrical signals from the current and voltage transducers were recorded on the PC equipped with the NI DAQ 6036 measuring card. The analyzed radiation was fed into the CCD spectrophotometer by means of a standard fibre optics. A spectrophotometer card PCI 2000 ISA-A (Ocean Optics Inc.) was used in this research. The output of each pixel is converted to an electrical current which represents the amount of the energy that has fallen on each pixel in a relative manner.

Figure 19 shows the different influence of the welding current intensity on the amplitudes, additive constants and widths (FWHM) of the Lorentz functions that fit the best spectral peaks of the arc light. One can see that the influence manifests in different ways in the cases of the different spectral peaks. Generally, the welding current intensity strong influences the additive constants and amplitudes of the peaks in the spectral range from 400 nm to 500 nm. Figure 19d shows the dependence of the best fitted additive constants on intensity of the current in the welding process of the clean mild steel S 235 (I=104 A; U=16,5 V).

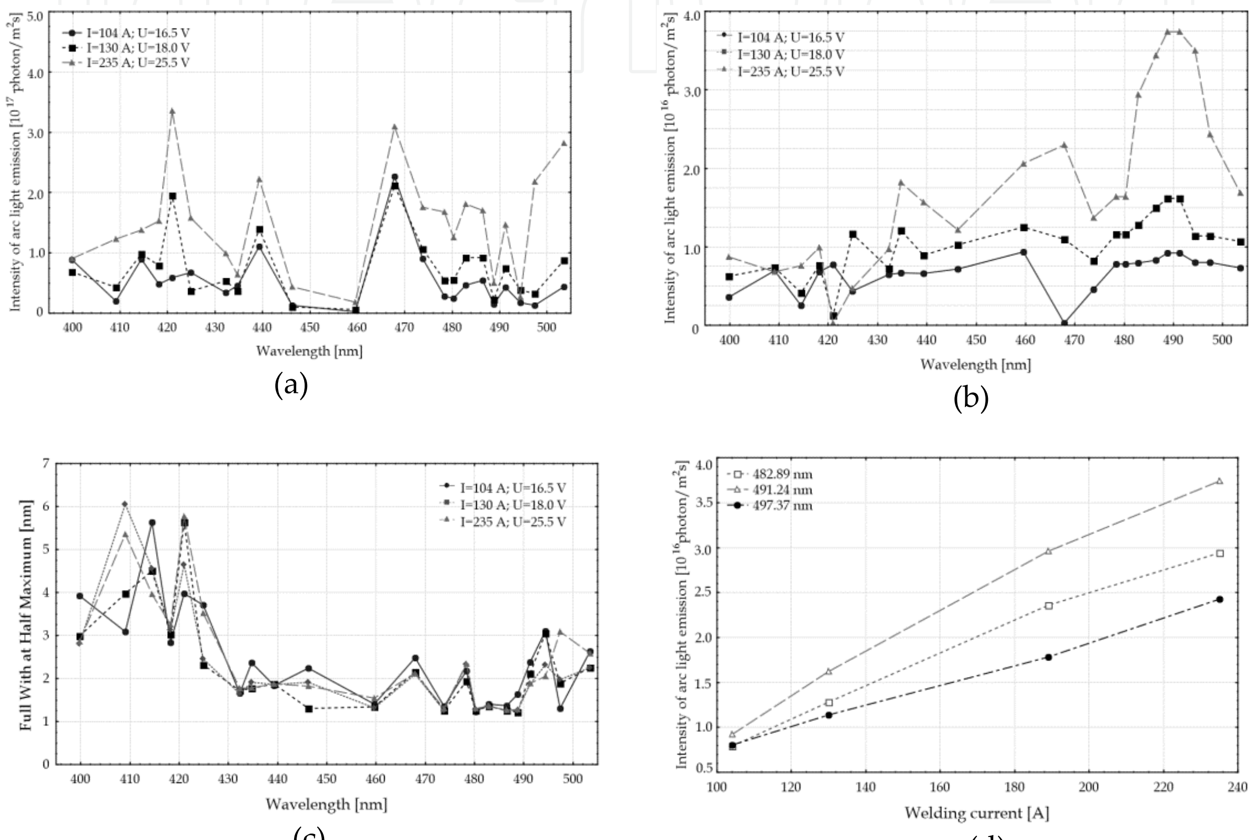

Figure 19. (a) influence of the welding current intensity on the amplitudes, (b) the values of additive constant in formula (3), (c) FWHM and (d) intensity of single emission lines,

Investigations on the effect of imposed disturbances, in the form of paint or grease layers on the plate surface, on the intensity of the MAG arc light radiation in the visible range, have been performed. The mild steel S 235 as the welding plate and the 1,2 mm diameter SG2 type welding wire were used. Experiments were performed with shielding gas 82% Ar and 18 % CO_2. The plate surface was clean, covered with oil paint or covered with a machine grease. It was found that both the paint and grease layer influence the recorded spectral characteristics of the MAG welding light radiation. Figure 20 presents the different influence of the existence of paint on the welded plate on the amplitudes, additive constants and the widths of the Lorentz functions that fit the best spectral peaks of the arc light. One can see that the influence manifests in different ways in the cases of the different spectral peaks.

The presented investigations show that the low resolution spectral characteristics of the arc light emission registered with CCD device can be applied for the purpose of monitoring of the welding process. The arranged measuring stand has made it possible to record the visible spectrum of the radiation of the welding arc within the range of wavelengths from 380 nm to 780 nm. The measuring stand comprised a spectrophotometer, a computer recording the results of the measurements and a device for mechanized welding.

It was found that the spectral distribution of a single peak in the low resolution spectral characteristics can be best fitted with the Lorentz function. In the recorded spectrum of the welding arc light emission, separation of the ionic or atomic lines is not possible. However, the correlation between the parameters of the fitted Lorentz function and welding parameters (i.e. welding current) was obtained. The Lorentz function parameters depend also on the disturbances in the MAG welding process, e.g. their values are different in the cases of clean and painted surface of the welded mild steel S 235 plate.

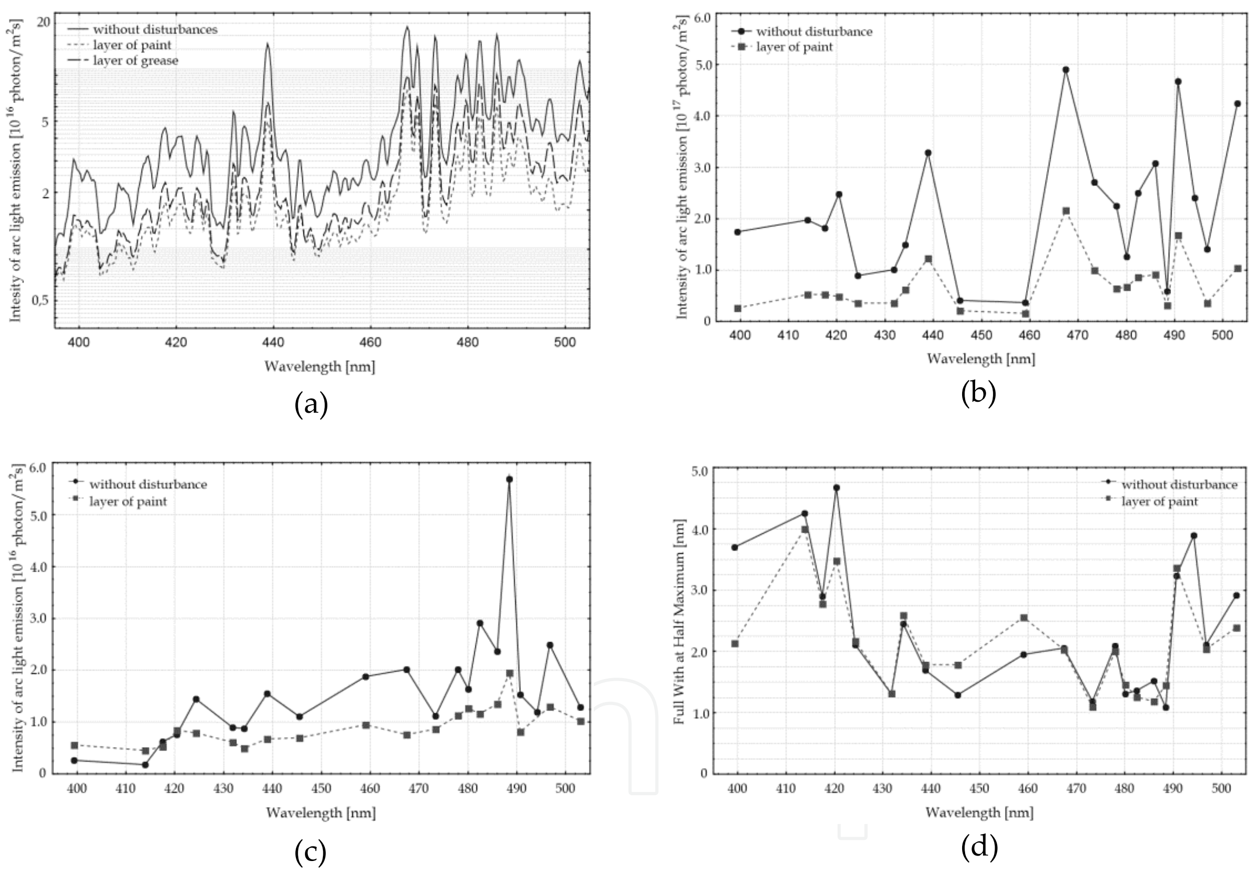

Figure 20. (a) the influence of disturbances on the MAG welding arc light spectrum (I=169 A, U=19,7 V) (b) influence of paint on the welded plate on the amplitudes, (c) the values of additive constant in formula (3) and (d) FWHM (Attention: curves presented in the figure cannot be interpolated)

5. Summary

Modern monitoring methods of the welding processes are inherent in each automatics and robotics production system. These systems detect very rapidly any incorrectly made weld joints during manufacturing and this way decreases the costs of production. That means possibility of detecting of any faulty parts without very costly nondestructive examinations. At present very popular conventional monitoring methods of the welding processes, based on measurements of the welding current and arc voltage in many cases are inefficient and are replaced or/and completed by nonconventional monitoring methods.

One of the most popular nonconventional monitoring method is sensing system based on the arc light emission. The main aim of these investigations was to check the possibilities of applying the visible radiation of the welding arc for the purpose of monitoring of the quality of the welding process.

The arranged measuring stand made it possible to record the visible spectrum of the radiation of the welding arc within the range of the wavelengths from 380 nm to 780 nm. The measuring stand comprised a spectrophotometer, a computer recording the results of measurements and a device for mechanized welding.

Results of the performed investigations in the field of measurement of light radiation intensity during TIG and MIG/MAG welding, shown in this chapter, indicate that this signal can be used for the monitoring of the welding process quality. The experience gained during these investigations allows for further research on the welding arc radiation phenomenon. The obtained knowledge increases the possibilities of using the signal for on-line monitoring of the welding process on the automated and robotized stands. The analysis of the spectrum of the welding arc radiation should help to develop the new vision sensor in the arc welding.

The investigations are continued in the many research centers, and cover the following issues:

- utilize the artificial intelligence method to estimate the stability of the welding process,
- develop the filtering method, and methodology to signal analysis in time, and frequency domain,
- laser diagnostic on the welding arc in the TIG and MIG/MAG methods, develop method of measurement of the arc light emission in many points simultaneously, and many others.

Author details

Marek Stanisław Węglowski
Instytut Spawalnictwa (Institute of Welding), Poland

6. References

Zhang, Y.M. (2008). *Real-time weld process monitoring*. Woodhead Publishing in Materials, ISBN 978-1-84569-268-1, Cambridge, England

Blakeley, P. J. (1990). Who should be using arc monitoring? *Welding and Metal Fabrication,* Vol. 58, No 6, pp. 268-272, ISSN 0043-2245

Siewert, T., Madigan, B. (1992). Through the arc sensing for measurement Gas Metal Arc weld quality in real time. *Materials Evaluation*, Vol. 50, No 11, pp. 1314-1318, ISSN 0025-5327

Chen, X. Q. (2002). *Advanced automation techniques in adaptive material processing*, Word Scientific Publishing, ISBN 981-02-4902-0, Rever Edge, New Jersey, USA.

Pan, J. (2003). *Arc welding control*. Woodhead Publisher Limited, ISBN 0-8493-1772-X, Cambridge, England.

Kim, J. W., Na, S. J. (1991). A study on an arc sensor for Gas Metal Arc welding of horizontal fillets. *Welding Journal*, Vol. 70, No 8, pp. 216s-221s, ISSN 0043-2296

Johnson, J. A., Carlson, N. M., Smartt H.B., et al (1991). Process control of GMAW: sensing of metal transfer mode. *Welding Journal*, Vol. 70, No 4, pp. 91s-99s, ISSN 0043-2296

Modenesi, P. J., Nixon, J. H. (1994). Arc instability phenomena in GMA welding. *Welding Journal*, Vol. 73, No 9, pp. 219s-224s, ISSN 0043-2296

Luksa, K. (2006). Influence of weld imperfection on short circuit GMA welding arc stability. *Journal of Materials Processing Technology*, Vol. 175, pp. 285-290, ISSN 0924-0136

Guu, A. C., Rokhlin, S. I. (1992). Arc welding process control using radiographic sensing. *Materials Evaluation*, Vol. 50, No 11, pp. 1344-1348, ISSN 0025-5327

Fan, H. Ravala, N. K., Wikle III, H. C., et al. (2003). Low-cost infrared sensing system for monitoring the welding process in the presence of plate inclination angle. *Journal of Materials Processing Technology*, Vol. 140, No 1-3, pp. 668-675, ISSN 0924-0136

Carlson, N. M., Johnson, J. A. (1992). Ultrasonic NDT methods for weld sensing. *Materials Evaluation*, Vol. 50, No 11, pp. 1338-1343, ISSN 0025-5327

Taylor-Burge, K. L., Harris, T. J. (1993). The real time analysis of acoustic weld emission using neural networks, *Proc. of the International Conf. on the Joining of Materials JOM-6* ed. Rasmus Knudsens Vej, pp. 60-67. Helsingor, Denmark

Saini, D., Floyd, S. (1998). An investigation of Gas Metal Arc welding sound signature for on-line quality control. *Welding Journal*, Vol. 77, No 4, pp. 172s-179s, ISSN 0043-2296

Luksa, K. (2003). Correspondence between sound emission generated in GMA [MIG/MAG] welding process and signals registered in the arc circuit. *Welding International*, Vol. 17, No 6, pp. 438-441, ISSN 0950-7116

Smith, J., Lucas, B. (1999). Putting intelligence into welding – rule based systems, fuzzy logic and neural networks. *Welding & Metal Fabrication*, Vol. 67, No 10, pp. 7-9, ISSN 0043-2245

Amin, M., Naseer, A. (1987). Synergic control in MIG welding – parametric relationship for steady DC open arc and short circuiting arc operation. *Metal Construction*, Vol. 19, No 1, pp. 22-28, ISSN 0026-0541

Kang, Y. H., Na, S. J. (2003). Characteristics of welding and arc signal n narrow groove GMAW using electromagnetic arc oscillation. *Welding Journal*, Vol. 82 No 5, pp. 93s-99s, ISSN 0043-2296

Lu, W., Zhang, Y. M. (2004). Sensing of weld pool surface using non-transferred plasma charge sensor. *Measurement Science and Technology*, Vol. 15, No 5, pp. 991-999, ISSN 0957-0233

Zheng, B., Wang, H. J. (2000). Control for weld penetration in VPPAW of aluminum alloys using the front weld pool image signal. *Welding Journal*. 70 (12): 363-s to 371-s, ISSN 0043-2296

Zhang, Y. M., Wu, L. (1993). Determination joint penetration in GTAW with vision sensing of weld face geometry. *Welding Journal*, Vol. 72, No 10, pp. 463s-469s, ISSN 0043-2296

Li, P. J., Zhang, Y. M. (2001). Precision Sensing of Arc Length in GTAW Based on Arc Light Spectrum. *Journal of Manufacturing Science and Engineering*, Vol. 123, No 1, pp. 62-65, ISSN 1087-1357

Wang, Q. L., Li, P. J. (1997). Arc light sensing of droplet transfer and ist analysis in pulsed GMAW processes. *Welding Journal*, Vol. 76, No 11, pp. 458s-469s, ISSN 0043-2296

Weglowski, M. St. (2007). Utilization of the arc light emission emitted during TIG welding to monitoring this process. *Archives of Mechanical Technology and Automation PAN*, Vol. 27, No 1, pp. 103-112. (in Polish), ISSN 1233-9709

Yoo, C. D., Yoo, Y. S., and Sunwoo H.K. (1997). Investigation on arc light intensity in gas metal arc welding. Part 1: relationship between arc light intensity and arc length. *Proceeding of the Institution of Mechanical Engineers. Part B: Journal of Engineering Manufacture*, Vol. 211 (B5), pp. 345-353, ISSN 0954-4054

Yoo, C. D., Yoo, Y. S., and Sunwoo H. K. (1997). Investigation on arc light intensity in gas metal arc welding. Part 2: application to weld seam tracking. *Proceeding of the "Institution of Mechanical Engineers. Part B: Journal of Engineering Manufacture*, Vol. 211 (B5), pp. 355-363, ISSN 0954-4054

Ancona, A., Lugara,P.M., Ottonelli,F., Catalano, I.M. (2004). A Sensing Torch for On-line monitoring of the Gas Tungsten Arc Welding Process of Steel Pipes. *Measurement Science and Technology*, Vol. 15, No 12, pp. 2412-2518, ISSN 1361-6501

Sadek, C.A., Diogo, D.S.M., Marcelo, S.M. (2006). Emission Spectrometry Evaluation in Arc Welding Monitoring System. *Journal of Materials Technology*, Vol. 179, No 1-2, pp. 219-224, ISSN 0924-0136

Li, Z. Y., Wang, B., Ding, J.B. (2009). Detection of GTA Welding Quality and Disturbance Factors with Spectral Signal of Arc Light. *Journal of Materials Processing Technology*, 2009, Vol. 209, No 10, pp. 4867-4873, ISSN 0924-0136

Mirapeix, J., Cobo, A., Fernandez, S., Cardoso, R., Lopez Higuera, J.M. (2008). Spectroscopic Analysis of the Plasma Continuum radiation for On-line Arc-welding Defect Detection. *Journal of Physics D: Applied Physics*, Vol. 41, No 3, pp. 135202–135210, ISSN 1361-6463

Johnson, C.A., Sciaky, A.M. (1966). *System for controlling length of welding arc*, Patent US, nr 3236997

Zhang, Y.M., Li, P.J. (2001). Precision sensing of arc length in GTAW based on arc light spectrum. *Journal of Manufacturing Science and Engineering*, Vol. 123, No 2, pp. 62-65, ISSN 1087-1357

Garcia-Allenda, P.B., Mirapeix, J., Conde, O.M., Cobo, A., Lopez-Higuera, J.M. (2008). Arc welding spectroscopic monitoring based on feature selection and neutral networks. *Sensors*, Vol. 8, No 10, 6496-6506, ISSN 1424-8220

Pattee, H.E, Myers L.B., Evans R.M., Monroe R.E. (1973). Effect of Arc Radiation and Heat on Welders. *Welding Journal*, Vol. 52, pp. 297s-308s. ISSN: 0043-2296

Hinrichs J.F., (1978). Radiation and arc welding: New data to enhance safety. *Welding and Metal Fabrication*, Vol. 51, pp. 102-103, ISSN 0043-224

Marzec, S., Janosik, E. (1995). Influence of arc radiation of health of welder Wpływ promieniowania łuku spawalniczego na organizm spawacza. *Builetyn of Welding Institute*, Vol. 39, No 6, 33-37, ISSN 0867-583X

Quigley, M. (1977). Physics of the welding arc. *Welding and Metal Fabrication*, Vol. 9, No 12, pp. 619-625, ISSN 0043-2245

Glickstein, S. (1976). Temperature measurements in a free burning arc. *Welding Journal*, Vol. 55, No 8, pp. 222s-229s, ISSN 0043-2296

Huddlestone, R.H., Leonard, S.L. (1965). *Plasma diagnostic techniques*. Academic Press, New York, USA

Szymański, A. (1991). *Spectroscopic and Computer Modeling Investigations of a Laser-Sustained Plasma*. Institute of Fundamental Technological Research Works, Polish Academy of Sciences, Warsaw, 30/1991

Petrie, T.W., Pfender, E. (1970). The influence of the cathode tip on temperature and velocity fields in a GTA. *Welding Journal*, Vol. 49, No 12, pp. 588s-596s, ISSN 0043-2296

Etemadi, K., Pfender, E. (1982). Computer – controlled plasma emission spectroscopy. *Review of Scientific Instruments*, No 2, pp. 255-257, ISSN 0034-6748

Lee, C.W., Na, S.J. (1996). A study on the influence of reflected arc light on vision sensors for welding automation. *Welding Journal*, Vol. 75, No 12, pp. 379s-387s, ISSN 0043-2296

Yu. J.Y., Kim. J.I., Na. S.J. (2003). Influence of reflected arc light on vision sensor for automatic GTAW systems. *Welding Journal*, Vol. 82, No 2, pp. 36s-42s, ISSN 0043-2296

Hinrichs, J.F. (1978). Radiation and arc welding: New data to enhance safety. Welding and Metal Fabrication, vol. 51, No. 2, pp. 102–103, ISSN 0043-2245

Farmer, A.J.D., Haddad, G.N. (1984). Local thermodynamic equilibrium in free-burning arcs in argon. *Applied Physics Letters*, Vol. 45, No 1, pp. 24-25, ISSN 0003-6951

Grove, L., Loseke, W.A., et al (1970). Development of portable direct reading spectrometer to monitor oxygen-hydrogen containing contaminants in gas tungsten-arc process shields. *Welding Journal*, Vol. 49, No 11, pp. 538s-545s, ISSN 0043-2296

Wang, Q.L., Li, P.J. (1997). Arc light sensing of droplet transfer and its analysis in pulsed GMAW processes. Welding Journal, Vol. 76, No 11, pp. 458-469, ISSN 0043-2296

Cho, Y.T., Na, S.J. (2005). Application of Abel inversion in real-time calculation for circularly and elliptically symmetric radiation sources. *Measurement Science and Technology*, Vol. 16, pp. 878-884, ISSN 0957-0233

Fan, H.G., Na, S.J., Shi, Y.W. (1997) Mathematical model of arc in pulsed current gas tungsten arc welding. *Journal of Physics D: Applied Physics*, Vol. 30, pp. 94-102, ISSN 0022-3727

Kang, Y.H., Na, S.J. (2002). A study on the modeling of magnetic arc deflection and dynamic analysis of arc sensor. *Welding Journal*, Vol. 81, No 1, pp. 8s-13s, ISSN 0043-2296

Ogawa, Y. (2004). Effect of active flux on anode reaction. Dokument MIS XII-1797-0

Zielińska S. (2004). *Physical properties of MIG/MAG plasma*. Doctoral thesis. Institute of Physics, Jagiellonian University, Krakow, Poland

Kończak, S., Nowak, M. (1981). The estimation of semiconductor parameters using least squares in photomagnetoelectric investigation. *Physica Status Solidi A - Application and Materials Science*, Vol. 63, pp. 305-311, ISSN 0031-8965

Węglowski, M. St. (2010), *Utilization of the arc light emission emitted by an electric arc to monitor the TIG process*. Doctoral thesis, AGH University of Science and Technology, Krakow, Poland

Węglowski, M.St. (2008). Modeling and analysis of arc light spectrum in GMAW. *Welding Journal*, Vol. 87, No 8, pp. 212-218, ISSN 0043-2296

Węglowski, M.St. (2009). Measurement of arc light spectrum in the MAG welding method. *Metrology and Measurement Systems PAN*, Vol. 16, No 1, 143-159. ISSN 0860–8229.

Węglowski, M.St., Zhang, Y.M. (2010). Relationship between welding conditions and intensity of arc light emission in GMAW. *Proceedings of the 5th International Conference on Advances in Production Engineering APE'2010*, Warsaw University of Technology, Warsaw, pp. 215-224, ISBN 978-83-7204-903-2